ACS Catalysis

Letter

pubs.acs.org/acscatalysis

Defect Sites in H_2-Reduced TiO_2 Convert Ethylene to High Density Polyethylene without Activator

Caterina Barzan, Elena Groppo,* Silvia Bordiga, and Adriano Zecchina

Department of Chemistry, INSTM and NIS Centre, University of Torino, Via Quarello 15 A, Torino 10135, Italy

Supporting Information

ABSTRACT: We show the unprecedented potential of commercially available TiO_2 materials reduced in H_2 (H_2-reduced TiO_2) in the conversion of ethylene to high density polyethylene (HDPE) under mild conditions (room temperature, low pressure, absence of any activator), with the consequent formation of HDPE/TiO_2 composites, which have been characterized by electron microscopy. Combination of UV−vis and IR spectroscopies allows one to demonstrate that ethylene polymerization occurs on Ti^{4-n} defect sites, which behave as shallow-trap defects located in the band gap and, differently from the active sites in the widely used Ziegler−Natta catalysts, do not contain any alkyl (Ti−R) or hydride (Ti−H) ligands. These results represent a step forward the understanding of ethylene polymerization mechanism and open valuable perspectives for commercial TiO_2 materials as catalysts for polyethylene production under mild conditions.

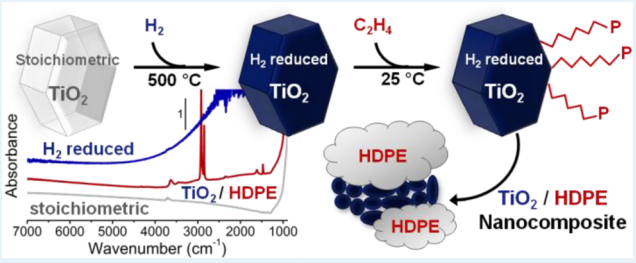

KEYWORDS: *H_2-reduced TiO_2, Ziegler−Natta catalysts, defect sites, ethylene polymerization, HDPE*

Titanium dioxide (TiO_2) is one of the most investigated materials in the field of photocatalysis,[1] photovoltaics[2] (coupled with organic dies), and water splitting.[3] Defective TiO_2 is even more attractive compared with stoichiometric TiO_2 because of its narrower band gap (<3 eV), which allows the absorption of visible light and a moderate conductivity. Several approaches have been proposed to introduce defects into TiO_2, with the aim of engineering the band gap and improving solar light harvesting. The most popular methods involve either the introduction of dopants (metals, nonmetals,[4−7] or self-dopant Ti^{3+} species[8]) or the generation of oxygen vacancies through annealing (outgassing at high temperatures in UHV)[9] or reduction in hydrogen atmosphere.[10,11] Recently, black TiO_2 nanoparticles with 1.0 eV band gap were obtained through high-pressure hydrogenation starting from crystalline TiO_2[1] and amorphous TiO_2,[12] respectively. The authors ascribe the observed color and, therefore, the narrowed band gap to the synergistic presence of surface disorder and oxygen vacancies in bulk and surface positions. These black TiO_2 nanoparticles are highly stable in air for over 10 months because of the replenishment of oxygen in the surface vacancies, leaving a unique crystallinity core/disordered shell morphology. Black TiO_2 shows enhanced photocatalytic activity with respect to stoichiometric TiO_2, for example, in decomposition of methylene blue or in water splitting reaction upon irradiation with UV−vis light. TiO_2 presenting surface and subsurface oxygen vacancies also play an active role in catalytic reactions involving the activation of water, alcohols, acetone, and formaldehyde without the need for light irradiation.[13−15]

In our view, the presence of Ti^{4-n} sites at the surface of reduced TiO_2 was attractive because of its similarity with the reduced Ti sites active in olefin polymerization and oligomerization. As a matter of fact, reduced Ti sites in interaction with an aluminum−alkyl activator are the active species in the well-known $TiCl_x$-based heterogeneous Ziegler−Natta (ZN) catalysts,[16−19] which have a dominant share of polypropylene and polyethylene production. It is also known that $TiCl_2$ (where Ti has a 2+ oxidation state) polymerizes ethylene in absence of any activator.[20] Finally, homogeneous aryloxy- and alkoxy-Ti^{2+} organometallic complexes selectively oligomerize ethylene to mainly 1-butene (alphabutol process) and other light olefins.[21−24] Inspired by these examples and on the basis of our experience in the field of characterization of heterogeneous catalysts for ethylene polymerization,[25−32] we explored the potential of reduced TiO_2 materials in the oligomerization/polymerization of ethylene. Herein, we report the first observation of the occurrence of ethylene polymerization under mild conditions (room temperature, low pressure, absence of any cocatalyst) at the surface of commercially available TiO_2 materials (Aldrich nanoanatase, nanorutile, and Degussa P-25) reduced in H_2 atmosphere. We demonstrate that a high-density polyethylene (HDPE) is obtained, characterized by a high degree of crystallinity.

Briefly, the activation procedure was as following: (i) All TiO_2 samples were first degassed at 773 K in dynamic vacuum for several hours, followed by a treatment in oxygen at the same

Received: January 15, 2014
Revised: February 11, 2014
Published: February 14, 2014

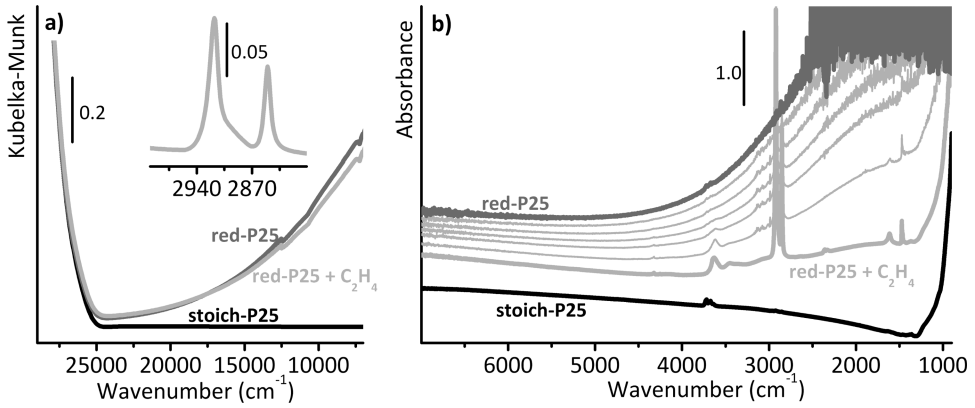

Figure 1. DR UV−vis−NIR (part a) and FT-IR (part b) spectra of stoichiometric P-25 activated at 773 K in O_2 (bold black) and reduced in H_2 atmosphere at 773 K (bold dark gray) and of the last sample after 12 h of exposure to ethylene (bold light gray). The series of spectra in light gray were collected while ethylene polymerization occured. The inset in part a shows the IR spectrum (collected in ATR mode) in the $\nu(CH_2)$ region of the PE obtained on H_2-reduced P-25 during the DR UV−vis measurement.

temperature (1 h), to remove organic pollutants possibly present at the surface and to provide stoichiometric TiO_2 (hereafter, stoich-TiO_2). (ii) A reduction step was carried out in hydrogen atmosphere (pressure of 200 mbar) at 773 K for 1 h. (iii) H_2 was pumped out at 773 K, and the samples were rapidly cooled to room temperature (hereafter, red-TiO_2). We would like to note that the reduction conditions employed herein are milder than those leading to the black TiO_2 reported in the literature, which requires high H_2 pressure (more than 10 bar).[1] All the steps were conducted in a quartz tube to avoid possible contamination, as recently shown in the literature.[33] All reduced samples show a blue color. At that point, ethylene was admitted into the reaction cell at room temperature and low pressure (lower than 200 mbar). A gradual decrease in the ethylene equilibrium pressure was observed in all the cases, demonstrating that ethylene polymerization occurs. Remarkably, the kinetic behavior is reproducible upon new admission of ethylene for several times, demonstrating that the catalyst does not deactivate in the adopted experimental conditions. Reaction constants in the range of 5.0×10^{-3} to 1.0×10^{-2} s^{-1} $mol_{TiO_2}{}^{-1}$ were obtained, corresponding to an activity of about 7−15 g_{PE} $g_{TiO_2}{}^{-1}$ h^{-1} at room temperature and low pressure. It should be noticed that the activity values refer to grams of catalyst and not to the number of active sites, which are difficult to estimate. The activity data evaluated from the kinetics of the reaction were confirmed by analysis of the weight increase in the sample.

The observation of the reactivity of H_2-reduced TiO_2 materials toward ethylene under mild conditions prompted us to carry out a spectroscopic investigation to get information on the catalytic active sites and on the properties of the produced polymer. Hereafter, we will discuss in detail the results obtained on the Degussa P-25 sample; similar results were obtained on nanoanatase and nanorutile samples, as reported in the Supporting Information (SI). Figure 1a and b show the DR UV−vis−NIR (part a) and FT-IR (part b) spectra of stoichiometric P-25 (black curve, stoich-TiO_2), reduced in H_2 at 773 K (dark gray curve, red-TiO_2) and of H_2-reduced P-25 after ethylene polymerization at room temperature (bold light gray curve, red-TiO_2 + C_2H_4). The spectra of stoichiometric P-25 (black curves) are basically flat over most of the frequency region, except above 26 000 cm^{-1} (optical band gap) and below 1000 cm^{-1} (bulk vibrational modes). The weak IR absorption bands observed around 3650 cm^{-1} are assigned to ν(O−H) of surface titanol species. The position and intensity of these bands differ as a function of sample (nanoanatase, nanorutile, or Degussa P-25) and activation time.[34,35] Because titanols are not directly involved in ethylene polymerization reaction, these bands are not described in detail.

Upon H_2 reduction, a broad and featureless absorption appears throughout the whole visible, NIR, and MIR regions (dark gray spectra in Figure 1a and b), with a consequent drastic decrease in transmittance. This phenomenon has been widely studied[36−39] and is explained in terms of creation of shallow-trap defect sites (plausible Ti^{4-n} sites associated with oxygen vacancies) located in the band gap. Electrons are promoted from these defect sites to the conduction band upon absorption of light. The closer the defect is to the valence band, the higher the energy that is required to promote the electron in the conduction band. In contrast, radiation in the IR region induces small thermal excitations that promote electrons from defect states that are close to the conduction band. A high density of states provides a continuum of electronic excitations, resulting in a featureless absorption in the whole IR region over a wide energy range (known as Drude absorption). Such a property of reduced TiO_2 was exploited to build up sensors for oxidizing/reducing agents:[40] as a matter of fact, an oxidizing/reducing asdorbate can remove/inject electrons into the surface defect states, inducing a change of the absorption in the IR range. The effect of H_2 reduction on the UV−vis-NIR and IR spectra is similar for the three TiO_2 materials investigated in this work (see SI), although some differences merit a comment. In particular, the broad Drude absorption is shifted at higher energy (i.e., wavenumber) values for nanorutile, suggesting that defect sites are electronically more profound (i.e., not as close to the conduction band).

It is important to observe that the appearance of a broad absorption throughout the vis−NIR−MIR region is the only spectroscopic phenomenon observed upon H_2 reduction of TiO_2 materials. No other absorption bands, which could reveal the presence of H-containing surface specie (e.g., Ti−H), are observed. The case of H_2-reduced nanorutile is helpful in this context because it is transparent in the 2500−1100 cm^{-1} region, where titanium hydride species are expected to contribute. Similarly, no additional absorption bands are observed in the IR spectrum of P-25 only partially reduced in H_2 (i.e., treated in H_2 at 500 °C for short contact time).

dx.doi.org/10.1021/cs500057s | ACS Catal. 2014, 4, 986−989

When ethylene interacts with reduced P-25, the broad absorption in the NIR-IR region due to the delocalized electrons slowly decreases in intensity, suggesting that a fraction of Ti^{4-n} sites are reoxidized (light gray sequence of spectra in Figure 1b). This can be explained in terms of oxidative addition of ethylene to Ti^{4-n} sites, with consequent formation of Ti−R species (where R = alkyl chain), although a possible oxidant role of a few parts per million of oxygen in the ethylene feedstock cannot be ruled out. The phenomenon is much less evident in the UV−vis region (Figure 1b), providing evidence that reoxidation involves defect sites close to the conduction band, much more than those electronically more profound. Simultaneously, IR absorption bands characteristic of polyethylene grow at 2923−2854 cm^{-1} (asymmetric and symmetric $\nu(CH_2)$) and at 1472−1459 cm^{-1} (asymmetric and symmetric $\delta(CH_2)$), revealing that H_2-reduced P-25 catalyzes ethylene polymerization. Hence, the decrease in ethylene pressure observed as a function of time must be correlated with ethylene polymerization on the TiO_2 surface. Noticeably, no reaction takes place on stoichiometric TiO_2 under the same reaction condition, which means that the defect sites responsible for the ethylene polymerization are generated during the H_2-reduction treatment. The whole set of data discussed above suggest that the reaction likely occurs on defect sites electronically located in proximity of the conduction band, whereas those more profound in the band gap are not involved.

A close inspection to the IR spectra allows one to get information on the resultant polymer. Indeed, the absence of absorption bands due to CH_3 moieties ($\nu(CH_3)$ expected at 2965 and 2872 cm^{-1} and $\delta(CH_3)$ at 1379 cm^{-1}) is indicative of the formation of HDPE, a linear polymer with a negligible amount of branches, as confirmed by DSC data (see SI Figure S4).[41] A polyethylene having the same vibrational spectrum is obtained during the DR UV−vis experiment (as demonstrated by the IR spectrum collected in ATR mode on the same powder at the end of the UV−vis experiment; inset of Figure 1a). The full width at high maximum and the intensity ratio between the absorption bands at 1472 and 1459 cm^{-1} (due to $\delta(CH_2)$) demonstrate that the obtained HDPE is highly crystalline.

Finally, the morphology of the HDPE/TiO_2 composite material was investigated by HRTEM. A few representative images are shown in Figure 2. It is worth noticing that detection of a polymer phase on top of the regular TiO_2 crystals is not straightforward because of the poor contrast of the polymer with respect to TiO_2. At the adopted resolution, the H_2-reduced TiO_2 particles show a morphology and size distribution typical of Degussa P-25: the particles are regular and have polyhedral shapes, with flat terminations. Polyethylene is randomly distributed on top of the TiO_2 particles, forming an ill-defined phase (indicated by arrows in Figure 2). A thorough investigation of many regions of the sample revealed that polyethylene is present overall in the sample, most probably involving both anatase and rutile particles. This observation agrees with the fact that similarly reduced nanorutile and nanoanatase (characterized by different type of defects: deeper in the band gap for nanorutile, closer to the conduction band for nanoanatase) were also found to be active in ethylene polymerization (see SI). It is worth noticing that recent accurate HRTEM investigation have demonstrated that hydrogenated black TiO_2 nanocrystals show a crystalline-disordered core−shell structure;[42−44] however, the phenomenon observed herein contributes at a much larger dimensional scale: the "ill-defined phase" constitutes islands as large as 50 nm, which are by far much larger than the average dimension of TiO_2 particles.

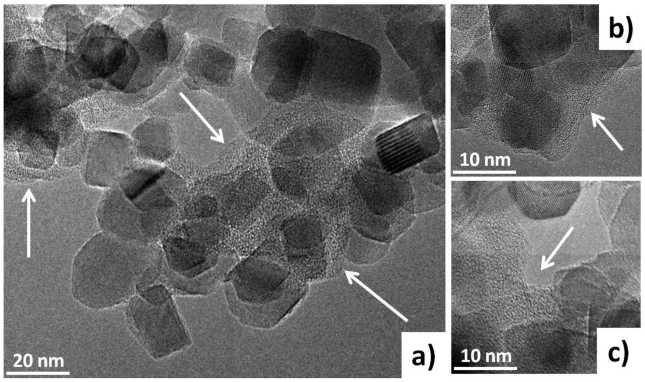

Figure 2. Representative HRTEM micrographs of H_2-reduced P-25 after ethylene polymerization occurred. Parts a, b, and c report three different images representative of the whole sample; the polyethylene phase is evidenced by white arrows.

In conclusion, the data shown herein demonstrate that commercially available TiO_2 samples can act as ethylene polymerization catalysts under mild conditions when reduced in H_2 at 773 K. Although the productivity is still low in comparison with the catalysts employed commercially for ethylene polymerization, TiO_2 has the advantage of being easy to handle, nontoxic, and widely available. Higher activity values could be achieved by increasing the fraction of active sites, for example, with TiO_2 materials having a higher surface area, or by using other reducing methods as well as by working at higher pressure and temperature. Therefore, the optimization of both catalyst properties and reaction conditions are potentially interesting in the field of polyethylene production. The exact nature and the amount of the active sites are still under investigation, but it can be safely stated that they are reduced Ti^{4-n} species that behave as shallow-trap defects located in the band gap and are responsible of the appearance of a broad absorption in the whole vis−NIR and MIR region.

Interestingly, the active Ti sites differ from the majority of $TiCl_x$-based heterogeneous catalysts for ethylene polymerization in two main aspects: (i) they do not have chlorine ligands in their coordination sphere, but only oxygen atoms; and (ii) they polymerize ethylene without any activator. In this respect, H_2-reduced TiO_2 materials are comparable to the Cr/SiO_2 Phillips catalyst, in which the active Cr−siloxy sites polymerize ethylene without any activator and for which the mechanism of initiation reaction is still an object of debate.[26,30,45−47] In the present case, the observation that a fraction of the Ti sites are reoxidized during ethylene polymerization reaction and the absence of any evidence for Ti−H (or Ti-R) species suggest that ethylene polymerization initiates through an oxidative addition. Future investigations will be devoted to the understanding of the reaction mechanism, with implications potentially useful to the whole community of researchers involved in olefin polymerization/oligomerization.

EXPERIMENTAL METHODS

The electronic and vibrational properties of stoichiometric TiO_2 (stoich-TiO_2) and reduced TiO_2 (red-TiO_2) samples were investigated by diffuse reflectance (DR) UV−vis−NIR

dx.doi.org/10.1021/cs500057s | ACS Catal. 2014, 4, 986−989

(Varian, Cary 5000) and transmission FT-IR (Bruker, Vertex 70) spectroscopy (Figure 1 and SI Figure S1). The same techniques were employed to monitor in situ the occurrence of ethylene polymerization, as frequently reported for other polymerization catalysts. The morphology of the TiO_2/polyethylene composite materials was determined by TEM (JEOL 3010-UHR; SI Figure S2), whereas the properties of the polymers were investigated by scanning electron microscopy (Zeiss evo50xvp; SI Figure S3) and differential scanning calorimetry (TA Instruments Q200; SI Figure S4) techniques.

■ ASSOCIATED CONTENT

Supporting Information

Vibrational and electronic spectra of H_2-reduced nanoanatase, nanorutile and P-25 reacted with ethylene, HR-TEM, SEM, and DSC study of the TiO_2/HDPE composites. This material is available free of charge via the Internet at http://pubs.acs.org.

■ AUTHOR INFORMATION

Corresponding Author

*E-mail: elena.groppo@unito.it.

Notes

The authors declare no competing financial interest.

■ ACKNOWLEDGMENTS

The work has been supported by FIRB (RBAP115AYN) and by Ateneo-Compagnia di San Paolo-2011-1A line, OR-TO11RRT5 projects. The authors thank Federica Franconieri for HRTEM and SEM images, and Giuseppe Spoto along with Lorenzo Mino for useful discussion.

■ REFERENCES

(1) Chen, X. B.; Liu, L.; Yu, P. Y.; Mao, S. S. *Science* **2011**, *331*, 746−750.
(2) Wang, G. M.; Wang, H. Y.; Ling, Y. C.; Tang, Y. C.; Yang, X. Y.; Fitzmorris, R. C.; Wang, C. C.; Zhang, J. Z.; Li, Y. *Nano Lett.* **2011**, *11*, 3026−3033.
(3) Chen, X. B.; Shen, S. H.; Guo, L. J.; Mao, S. S. *Chem. Rev.* **2010**, *110*, 6503−6570.
(4) Hoffmann, M. R.; Martin, S. T.; Choi, W. Y.; Bahnemann, D. W. *Chem. Rev.* **1995**, *95*, 69−96.
(5) Chen, X. B.; Burda, C. *J. Am. Chem. Soc.* **2008**, *130*, 5018−5019.
(6) Livraghi, S.; Chiesa, M.; Paganini, M. C.; Giamello, E. *J. Phys. Chem. C* **2011**, *115*, 25413−25421.
(7) Bjorheim, T. S.; Kuwabara, A.; Norby, T. *J. Phys. Chem. C* **2013**, *117*, 5919−5930.
(8) Zuo, F.; Wang, L.; Wu, T.; Zhang, Z. Y.; Borchardt, D.; Feng, P. Y. *J. Am. Chem. Soc.* **2010**, *132*, 11856−11857.
(9) Thompson, T. L.; Yates, J. J. T. *Chem. Rev.* **2006**, *106*, 4428−4453.
(10) Rekoske, J. E.; Barteau, M. A. *J. Phys. Chem. B* **1997**, *101*, 1113−1124.
(11) Barnard, A. S.; Zapol, P. *Phys. Rev. B* **2004**, *70*, article no. 235403.
(12) Naldoni, A.; Allieta, M.; Santangelo, S.; Marelli, M.; Fabbri, F.; Cappelli, S.; Bianchi, C. L.; Psaro, R.; Dal Santo, V. *J. Am. Chem. Soc.* **2012**, *134*, 7600−7603.
(13) Panayotov, D. A.; Yates, J. T. *Chem. Phys. Lett.* **2005**, *410*, 11−17.
(14) Xia, Y. B.; Zhang, B.; Ye, J. Y.; Ge, Q. F.; Zhang, Z. R. *J. Phys. Chem. Lett.* **2012**, *3*, 2970−2974.
(15) Xu, M. C.; Noei, H.; Fink, K.; Muhler, M.; Wang, Y. M.; Woll, C. *Angew. Chem., Int. Ed.* **2012**, *51*, 4731−4734.
(16) Albizzati, E.; Giannini, U.; Collina, G.; Noristi, L.; Resconi, L. Catalysts and Polymerizations. In *Polypropylene Handbook*; Moore, E. P. J., Ed.; Hanser-Gardner Publications: Cincinnati, OH, 1996; Chapter 2.
(17) Mulhaupt, R. *Macromol. Chem. Phys.* **2003**, *204*, 289−327.
(18) Corradini, P.; Guerra, G.; Cavallo, L. *Acc. Chem. Res.* **2004**, *37*, 231−241.
(19) Busico, V. *MRS Bull.* **2013**, *38*, 224−228.
(20) Kissin, Y. V. *Alkene Polymerization Reactions with Transition Metal Catalysts*; Kissin, Y. V., Ed.; Elsevier: Amsterdam, London, 2008; Vol. *173*.
(21) Suttil, J. A.; McGuinness, D. S. *Organometallics* **2012**, *31*, 7004−7010.
(22) Suttil, J. A.; McGuinness, D. S.; Pichler, M.; Gardiner, M. G.; Morgan, D. H.; Evans, S. J. *Dalton Trans.* **2012**, *41*, 6625−6633.
(23) McGuinness, D. S. *Chem. Rev.* **2011**, *111*, 2321−2341.
(24) Dixon, J. T.; Green, M. J.; Hess, F. M.; Morgan, D. H. *J. Organomet. Chem.* **2004**, *689*, 3641−3668.
(25) Groppo, E.; Seenivasan, K.; Barzan, C. *Catal. Sci. Technol.* **2013**, *3*, 858−878.
(26) Groppo, E.; Lamberti, C.; Bordiga, S.; Spoto, G.; Zecchina, A. *Chem. Rev.* **2005**, *105*, 115−183.
(27) Zecchina, A.; Groppo, E. *Proc. R. Soc. London, Ser. A* **2012**, *468*, 2087−2098.
(28) Groppo, E.; Damin, A.; Otero Arean, C.; Zecchina, A. *Chem.—Eur. J.* **2011**, *17*, 11110−11114.
(29) Barzan, C.; Groppo, E.; Quadrelli, E. A.; Monteil, V.; Bordiga, S. *Phys. Chem. Chem. Phys.* **2012**, *14*, 2239−2245.
(30) Groppo, E.; Lamberti, C.; Bordiga, S.; Spoto, G.; Zecchina, A. *J. Catal.* **2006**, *240*, 172−181.
(31) Seenivasan, K.; Sommazzi, A.; Bonino, F.; Bordiga, S.; Groppo, E. *Chem.—Eur. J.* **2011**, *17*, 8648−8656.
(32) Seenivasan, K.; Gallo, E.; Piovano, A.; Vitillo, J. G.; Sommazzi, A.; Bordiga, S.; Lamberti, C.; Glatzel, P.; Groppo, E. *Dalton Trans.* **2013**, *42*, 12706−12713.
(33) Danon, A.; Bhattacharyya, K.; Vijayan, B. K.; Lu, J.; Sauter, D. J.; Gray, K. A.; Stair, P. C.; Weitz, E. *ACS Catal.* **2012**, *2*, 45−49.
(34) Deiana, C.; Fois, E.; Coluccia, S.; Martra, G. *J. Phys. Chem. C* **2010**, *114*, 21531−21538.
(35) Mino, L.; Ferrari, A. M.; Lacivita, V.; Spoto, G.; Bordiga, S.; Zecchina, A. *J. Phys. Chem. C* **2011**, *115*, 7694−7700.
(36) Diebold, U. *Surf. Sci. Rep.* **2003**, *48*, 53−229.
(37) Szczepankiewicz, S. H.; Colussi, A. J.; Hoffmann, M. R. *J. Phys. Chem. B* **2000**, *104*, 9842−9850.
(38) Szczepankiewicz, S. H.; Moss, J. A.; Hoffmann, M. R. *J. Phys. Chem. B* **2002**, *106*, 2922−2927.
(39) Berger, T.; Sterrer, M.; Diwald, O.; Knozinger, E.; Panayotov, D.; Thompson, T. L.; Yates, J. T. *J. Phys. Chem. B* **2005**, *109*, 6061−6068.
(40) Baraton, M. I.; Merhari, L. *Nanostruct. Mater.* **1998**, *10*, 699−713.
(41) Chelazzi, D.; Ceppatelli, M.; Santoro, M.; Bini, R.; Schettino, V. *Nat. Mater.* **2004**, *3*, 470−475.
(42) Xia, T.; Chen, X. *J. Mater. Chem. A* **2013**, *1*, 2983−2989.
(43) Liu, L.; Yu, P. Y.; Chen, X.; Mao, S. S.; Shen, D. Z., *Phys. Rev. Lett.* **2013**, *111*, 065505.
(44) Lu, H.; Zhao, B.; Pan, R.; Yao, J.; Qiu, J.; Luo, L.; Liu, Y. *RSC Adv.* **2014**, *4*, 1128−1132.
(45) McDaniel, M. P. *Adv. Catal.* **2010**, *53*, 123−606.
(46) McGuinness, D. S.; Davies, N. W.; Horne, J.; Ivanov, I. *Organometallics* **2010**, *29*, 6111−6116.
(47) Liu, B.; Nakatani, H.; Terano, M. *J. Mol. Catal. A* **2002**, *184*, 387−398.